Chapter Three

Photorefractivity in poly(*N*-vinylcarbazole) based Composites

Abstract

Two novel photorefractive polymer composites have been developed, based on the well known photoconductor poly(N-vinylcarbazole) (PVK) sensitized with 2,4,7-trinitro-9-fluorenone (TNF) and the nonlinear optical (NLO) molecules 4-(diethylamino)nitrobenzene (EPNA) or 4-(hexyloxy)nitrobenzene (HONB). Using holographic and other complimentary techniques, the photorefractive nature of the light induced gratings in these materials is confirmed and net gain is demonstrated in the EPNA composite. The applicability of the standard theory of photorefractivity in the case of polymers is discussed. Finally, it is shown that the change in the refractive index arises partly due to the reorientation of the NLO molecules under the influence of the space charge field.

3.1. Introduction

In the last few years an increasing interest has been observed in the development of photorefractive polymer materials with possible applications in image processing and reversible dynamic holographic storage [1]. The first photorefractive polymer was an electrooptic polymer which was made photoconducting after doping with a hole transport agent [2]. Several other similar materials [3-5] as well as fully functionalized polymers [6,7] have been reported, all showing moderate performance. Subsecond grating response was demonstrated in one of them [3]. The various polymeric architectures, together with their advantages and drawbacks will not be outlined here, as they can be found in review articles [1,8,9].

Recently, net gain, high diffraction efficiency and a fast response time were observed in a PVK based photoconducting polymer, doped with the NLO molecule FDEANST[1] [10]. In this material, PVK plays a dual role, providing both the functionality of charge transport and the required mechanical stability. This approach has proven to be the most fruitful in terms of performance and several PVK based photorefractive polymers have been reported until today, doped with a variety of NLO molecules [11-16].

In order to explore the mechanism of photorefractivity in this class of materials, two novel composites were developed by doping PVK with the NLO molecules EPNA or HONB and small amounts of TNF, which functions as a sensitizer. Their properties were studied using holographic and other complimentary techniques and the results where discussed in view of the standard model for photorefractivity. Finally, the mechanism of the refractive index change in these materials was investigated.

The theory, the sample preparation procedures and the measuring techniques, together with sensitivity and accuracy considerations, have been discussed in the previous chapters. Here, only the most important experimental conditions are stated and some equations are repeated for the sake of completeness.

3.2. Results and discussion

The preparation of samples has been described in the previous chapter. Early results were obtained from casted films containing 39% wt. EPNA and 0.1% wt. TNF relative to PVK, with thicknesses around 65 μm. 100 μm thick sandwiched samples with 40% wt. EPNA or HONB and 0.1% wt. TNF relative to PVK were also studied. As the concentration of the NLO molecules was well below the limit where phase separation becomes visible (approximately 50% wt.), the optical quality of the samples

[1] 3-fluoro-4-(*N*,*N*-dithylamino)-β-nitrostyrene.

was good and did not degrade in time. The main reason for sample degradation was the tendency of the polymer film to stick off the ITO plate after a few days.

The glass transition temperature (T_g) of pure PVK is around 200 degrees. With the introduction of large quantities of a NLO molecule, plasticization is expected to take place [17]. The composite films would soften at a temperature around 100 degrees. Electrooptic measurements also indicate that the T_g is in this range (see below). Accurate measurements with differential scanning calorimetry (DSC) however were inconclusive, mainly due to the fact that the NLO molecules were subliming at elevated temperatures [18]. This sublimation problem was apparent in early attempts to expel residual solvent from the sample with prolonged heating. Since then, the sample preparation procedure (as described in the previous chapter), was designed to minimize the loss of the NLO molecules during heat treatment.

3.2.1. Optical absorption

In order to be advantageous for applications, a photorefractive material should have a large range of wavelengths where it can be used. Especially in the high density information storage devices, response in the blue side of the visible is preferable. From this point of view, PVK is a promising material for photorefractive applications. It can be processed into good optical quality films, which absorb in the ultraviolet region of the spectrum and with the addition of small amounts of a sensitizer like TNF, it exhibits photoconductivity throughout the visible. The wavelength range of PVK based photorefractive polymers is ultimately limited by the NLO molecules.

In all photorefractive polymers so far, π conjugated donor-acceptor molecules, are used to provide the electrooptic functionality. Their hyperpolarizability increases strongly with the length of the conjugated block [19] and for this reason, stilbenes or larger blocks are preferred. However, a trade-off is known to exist between the nonlinearity and the transparency of these molecules, meaning that the ones with the highest hyperpolarizability, show strong absorption in the visible. Although in some cases they act as sensitizers [20], illumination at, or near their absorption tail is not desirable: Permanent gratings with long response times observed in several photorefractive polymers have been attributed to photochemical reactions involving these molecules [10,21-23]. Moreover, for the achievement of net gain, the absorption should be kept at a minimum. For these reasons, the range of wavelengths used to study photorefractive polymers has been limited to the red-near infrared part of the spectrum. In DEANST[2] containing polymers for example, the onset of absorption is around 600 nm and permanent gratings have been observed at 633 nm [23].

[2] 4-*N*,*N*-(diethylamino)-β-nitrostyrene

From a transparency point of view, benzene derivatives seem attractive candidates as NLO molecules in photorefractive polymers. As can be seen in figure 3.1, the onset of absorption of EPNA (in $CHCl_3$ solution) is below 475 nm. In the same figure, the optical density of the PVK:TNF:EPNA starting solution used for the preparation of the sandwiched samples is plotted. This spectrum is the superposition of the spectra of PVK and EPNA solutions with the proper concentration (the absorption of TNF is too weak to be seen on this scale), indicating the absence of any reaction between these two compounds. However, a large wavelength range is still wasted, as the absorption of EPNA extends about 100 nm more than that of PVK. This waste is minimized when HONB is used as the NLO molecule (inset of figure 3.2), due to the fact that the alkoxy group is a weaker donor than the dialkylamino one.

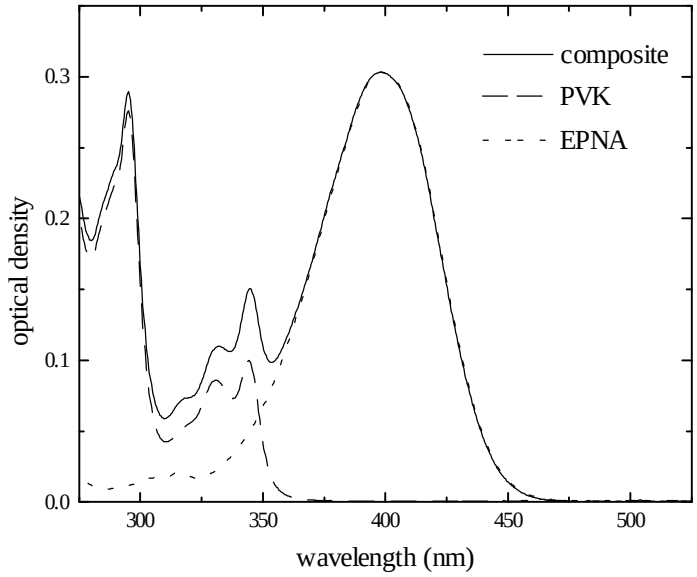

Fig. 3.1 *: Optical density of the PVK:TNF:EPNA starting solution compared with PVK and EPNA solutions of proper concentration, all in* $CHCl_3$.

The optical density of the sandwiched samples is shown in figure 3.2. Strong absorption for the EPNA composite begins about 500 nm, while the HONB composite offers 50 nm broader window towards the blue and it operates even at 488 nm [24]. The tail of the absorption is due to the PVK:TNF charge transfer complex and as expected, it is the same for both samples. Absorption at 633 nm is solely due to the PVK:TNF charge transfer complex. A formation of a charge transfer complex between PVK and

EPNA for example, can be ruled out, as samples that contain no TNF show no photorefractive response at 633 nm.

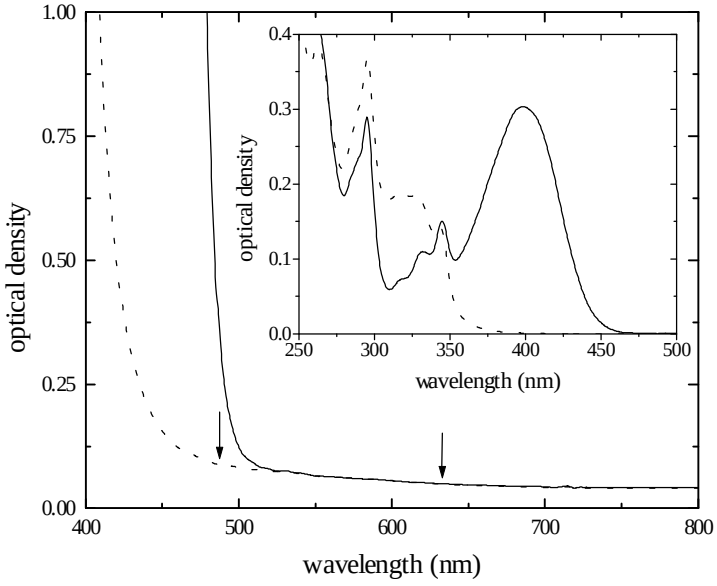

***Fig. 3.2** : Optical density of the sandwiched samples (solid line is for the EPNA composite and dotted line for the HONB composite). The two spectra are not corrected for reflections. The arrows indicate 488 and 633 nm. Inset : Optical densities of the PVK:TNF:EPNA (solid line) and PVK:TNF:HONB (dotted line) starting solutions in $CHCl_3$.*

3.2.2. Photoconductivity

The photoconductivity of PVK:TNF composites has been extensively studied in the past [25]. Absorption at wavelengths longer than 450 nm is attributed to the charge transfer complex which is formed between these two compounds [26]. For small amounts of TNF, the absorption of the composite increases linearly with TNF concentration [27]. The efficiency of charge generation is strongly electric field dependent and has been described on the basis of the Onsager theory of geminate recombination [26]. Both holes and electrons can be mobile in PVK:TNF composites, depending upon the composition. For low TNF concentration however, like in the composites that are discussed here, the electron mobility is practically zero [28]. Hole transport takes place via hopping, which is an activated process and the resulting

mobility is strongly electric field and temperature dependent [28]. More on the transport properties of PVK will be discussed in the next chapters.

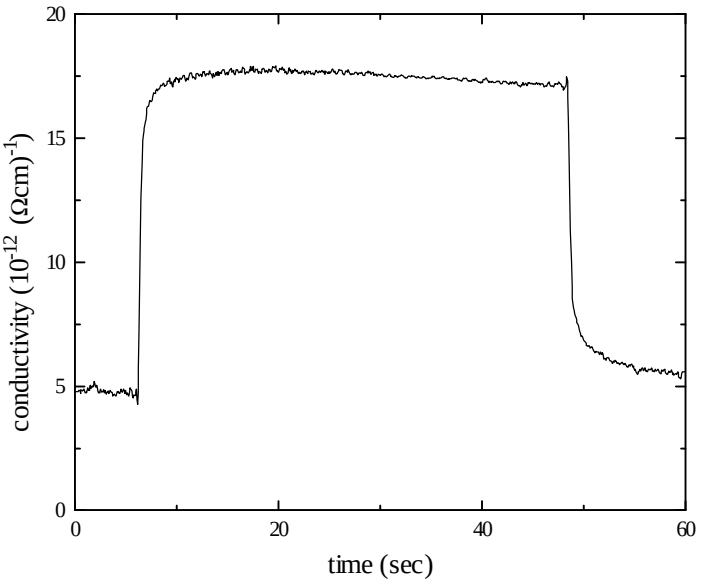

***Fig. 3.3** : Photocurrent response of the HONB composite. A He-Ne light beam with intensity of 40 mW/cm^2 was switched on for 40 seconds, at time equal ~6 sec. The electric field was 55 V/μm.*

The photocurrent response of the HONB composite is shown in figure 3.3. At time equal ~6 sec, a He-Ne light beam with intensity of 40 mW/cm^2 is switched on for 40 seconds, causing a reversible increase in conductivity, with the rise time of the photocurrent being in the subsecond range. Heating due to the laser beam can be safely ruled out, as the light intensity is very weak and the absorption of the sample very low. The corresponding sensitivity is in the order of $3 \cdot 10^{-10}$ (Ωcm)$^{-1}$/(W/cm^2), which is typical for photorefractive polymers [1].

3.2.3. Orientational mobility of the nonlinear optical molecules and electrooptic response of poly(*N*-vinylcarbazole) based photorefractive composites

The electrooptic properties of host-guest polymers are a subject of continuous research interest [29]. For a solution of NLO molecules in a polymer matrix, the electrooptic coefficient can be described as [30]:

$$r_{33} \propto \chi^{(2)}_{zzz} \propto N \beta_{333} \langle \cos^3\theta \rangle \quad (3.1)$$

where N is number density of the NLO molecules, β_{333} is the dominant component of their first hyperpolarizability tensor, θ is the angle between the molecular axis and the applied field and the symbol <> defines an average over all possible molecular orientations. A similar expression holds for r_{13}. Poling, which is necessary to remove the inversion symmetry and allow an electrooptic response, is usually carried out at temperatures close to the T_g, where the orientational mobility of the NLO molecules is relatively high. The poled structure is inherently unstable and the orientation of the NLO molecules tends to relax back to its random state, with a time constant that depends on the T_g, the architecture of the polymer and the poling procedure. Various approaches have been described in the literature, aiming at the maximization of the loading with NLO molecules, or the improvement of their orientational stability [29].

In host-guest polymers like the composites discussed here, the stability of the polar order at room temperature is rather poor [31]. As no physical linkage exists between the NLO molecules and the polymer backbone, relatively little constrain is present to prohibit their orientational relaxation. At the same time, in the case of photorefractive polymers, a high electric field is applied anyhow, in order to enhance charge generation and transport. The question arises, whether the same electric field can be used for efficient *in situ* poling of the NLO molecules at room temperature.

To check that, second harmonic generation (SHG) experiments were performed on casted samples, in the geometry described in the previous chapter. At the absence of an electric field, no signal could be measured, as a result of the centrosymmetric random arrangement of the NLO molecules. When the voltage on the needle exceeded 2 kV (the value above which corona discharge took place), SHG was immediately observed, indicating the ability of the NLO molecules to (partly) orient at room temperature. In figure 3.4, the square root of the SHG signal from a PVK:TNF:EPNA sample is plotted, exhibiting the expected quadratic behaviour with electric field[3]. SHG would essentially vanish as soon as the voltage was switched off. From the above it is clear that it is possible to induce a certain degree of molecular orientation at room temperature.

As with SHG, no electrooptic response could be measured on the sandwiched samples at the absence of an electric field. As the electric field was switched on, the electrooptic coefficient would reach a constant value and decay back to almost zero after the field was removed, within the temporal resolution of the measurement (a few seconds). A small magnitude tail, indicating some amount of residual orientation, would persist for a few minutes after prolonged poling. In figure 3.5, the electrooptic

[3] see equation (2.6).

coefficient r_{33}-r_{13} versus the electric field across the sample is shown for PVK:TNF:EPNA and PVK:TNF:HONB, measured at a modulation frequency of 1 kHz. A linear increase with the electric field is observed, in agreement with equation (3.1)[4]. The electrooptic effect in the EPNA composite is larger, which is expected due to the larger hyperpolarizability and dipole moment of this molecule [32]. Values in the pm/V range are typical for photorefractive polymers [1].

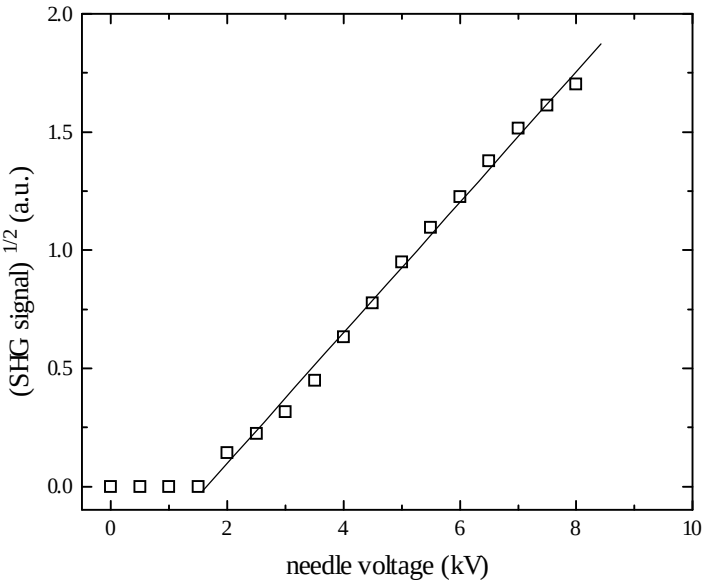

***Fig. 3.4** : Square root of the SHG signal from a PVK:TNF:EPNA casted sample as a function of the voltage on the needle. The offset on the horizontal axis is due to the existence of a threshold value for the establishment of the corona discharge. The line is a guide to the eye.*

The orientational mobility of the NLO molecules is expected to increase as the temperature is raised close to the T_g. This is shown in figure 3.6, where the electrooptic coefficient of the two composites increases in a linear-like fashion, reaching at 110 degrees a value that is about three times larger than that at room temperature. This behaviour is governed by the polymer matrix and as expected it is the same for both composites. Above 110 degrees, saturation and a slight decrease is observed. This effect has also been measured in other host-guest polymers at temperatures close or

[4] $\langle\cos^3\theta\rangle=\mu f(0)E_0/(5k_BT)$ (see equation (2.5)).

equal to T_g [33]. From the above it is clear that by lowering the T_g of the composites with the use of proper plasticizer, an increase of the electrooptic coefficient up to three times can be achieved.

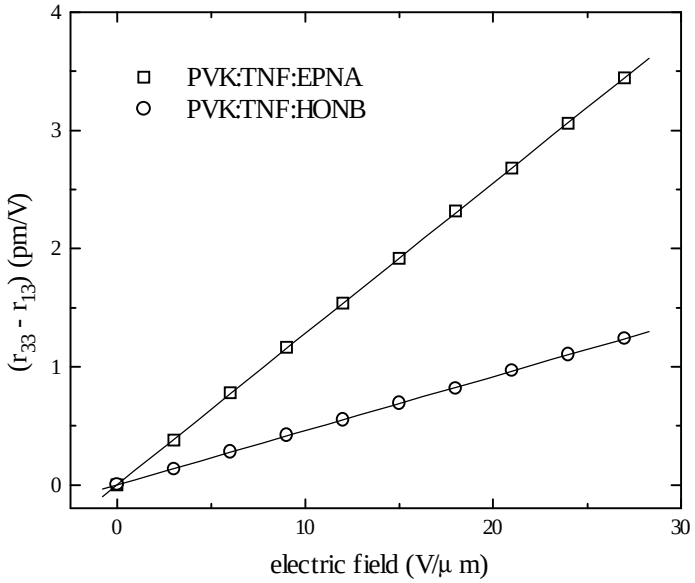

Fig. 3.5 *: The electrooptic coefficient r_{33}-r_{13} versus the electric field across the sample for the EPNA and the HONB composites, measured at a modulation frequency of 1 kHz and at room temperature. The lines are fits with slopes 0.127 and 0.045 (pm/V)/(V/μm) respectively. The actual value of the electrooptic coefficient showed a variation in the order of 10% from point to point on the same sample and 20% from sample to sample.*

In the presence of a dc electric field, Kerr effects can mimic a linear electrooptic response: The measured refractive index change, when Kerr effects are included, is given by [30]:

$$\Delta n \propto rE_T + sE_T^2 \qquad (3.2)$$

where r and s are the linear (Pockels) and quadratic (Kerr) electrooptic coefficients and E_T is the total electric field which is applied on the sample. Their main contribution is expected to arise due to birefringence which is induced from the reorientation of the NLO molecules in the ac field. Contrary to the linear electrooptic response, which is

electronic in origin (thus inherently fast), molecular reorientation is less likely to follow the ac field at high frequencies. This provides a means of separating the two effects.

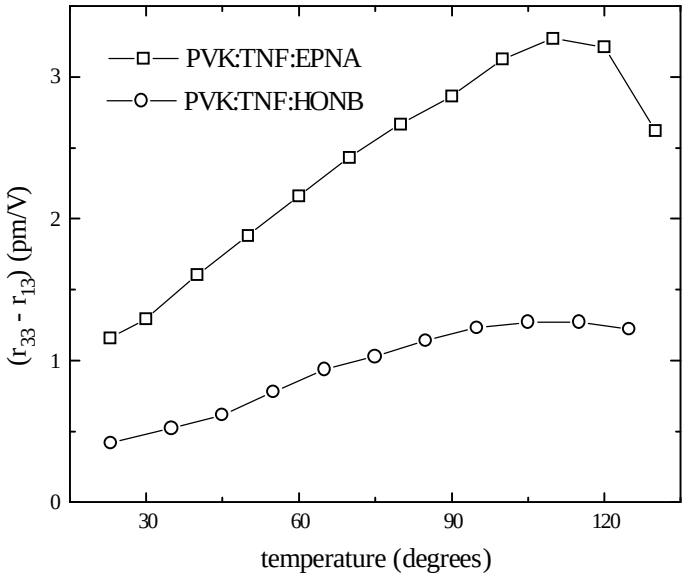

***Fig. 3.6** : The temperature dependence of the electrooptic coefficient for the two composites. The samples were heated up stepwise, with the electric field (9 V/μm) switched off during heating-up in order to avoid permanent poling at high temperatures.*

In figure 3.7, the frequency dependence of the electrooptic coefficient is shown for the two composites. A pronounced decrease of the electrooptic coefficient is noticed for both of them, indicating that molecular orientation is mainly responsible for the observed refractive index change. According to this, the electrooptic coefficients that are measured here are not the true ones in the standard sense, but correspond to:

$$r^* = r+2sE_{dc} \qquad (3.3)$$

where E_{dc} is the dc electric field. The exact magnitudes of r and s cannot be estimated as long as no plateau is observed in the frequency dependence, even up to 100 kHz. However, as it will be shown below, it is r^* that is important for the photorefractive effect. From now on, r^* will be referred to as the electrooptic coefficient, unless otherwise stated.

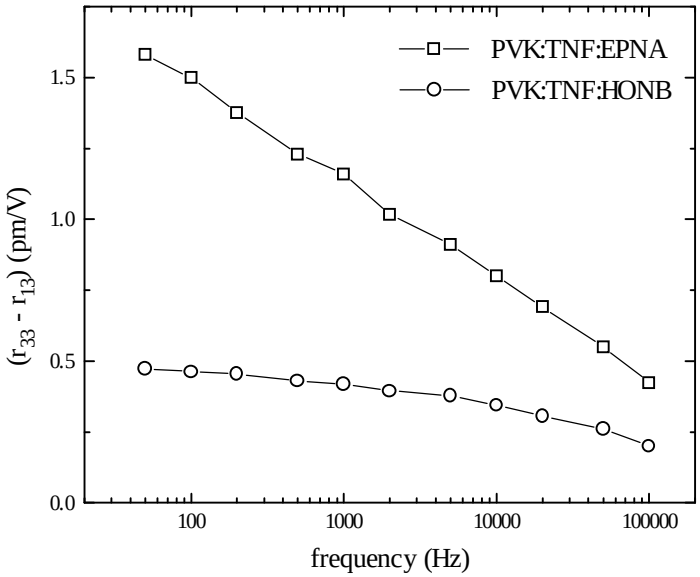

***Fig. 3.7** : The frequency dependence of the electrooptic coefficient r_{33}-r_{13} at room temperature. The electric field was 9 V/μm.*

3.2.4. Proof for the photorefractive nature of the observed gratings. Properties and comparison with the standard model

The coexistence of photoconductivity and electrooptic effect does not necessarily lead to photorefractivity. Traps suitable for sustaining a space charge field may not be present, or other types of light induced absorption or refractive index changes may dominate. Study with holographic techniques is necessary to identify the nature of the light induced gratings. Photochromic effects have usually long time constants, are non-reversible and show no electric field dependence. Thermal effects show no electric field dependence either. The gratings that were observed in PVK:TNF:EPNA and PVK:TNF:HONB had typical response time in the order of a second, were erasable and could only be written and read-out when an electric field was applied across the sample. Moreover, no gratings could be written when the two beams where incident in a symmetric geometry with respect to the sample normal, indicating that the electrooptic effect is responsible for the refractive index change[5]. Although the

[5] in a symmetric geometry r_{eff}=0.

combination of these characteristics provides strong evidence for the existence of photorefractivity, it is not a definite proof. In the PVK:TNF:Lophine 1 composite[6], reversible, electric field dependent, light induced refractive index gratings were attributed to a non-photorefractive mechanism, involving local photochemistry [34].

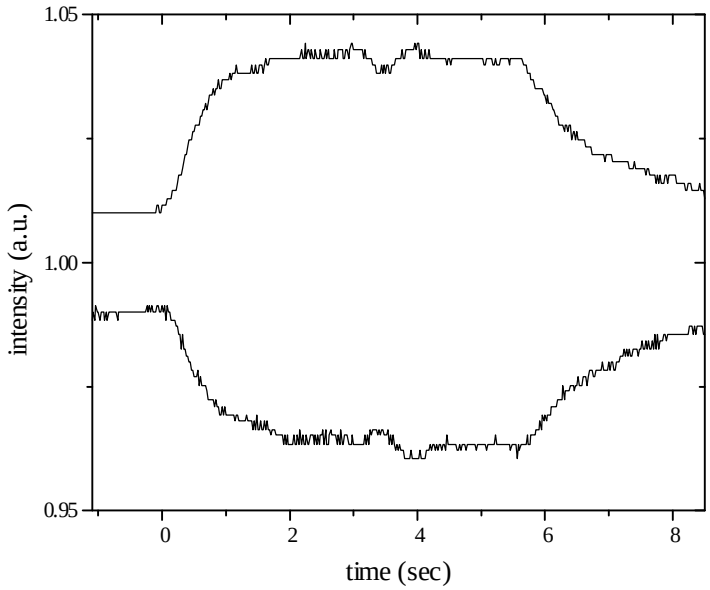

Fig. 3.8 *: Asymmetric energy exchange is observed in a PVK:TNF:EPNA sample when an electric field of 50 V/μm is switched on at time equal zero. The field is removed at approximately 5.6 sec.*

Unambiguous proof for the existence of photorefractivity is provided with the demonstration of a phase shifted refractive index grating. As it was discussed in the first chapter, the nonlocal character of photorefractive gratings results in a steady state asymmetric energy exchange between the two beams that write it. In figure 3.8, this is shown to be the case in PVK:TNF:EPNA. At time equal zero the electric field is switched on instantly, causing energy to be transferred from one beam to the other. This is the signature of the photorefractive effect in polymers. Under the influence of the electric field, the EPNA molecules adopt a non centrosymmetric arrangement and the sample becomes electrooptic. At the same time, charge generation and transport are enhanced and the space charge field begins to grow, giving rise to the photorefractive

[6] Lophine 1 is 2-(4-nitrophenyl)-4,5-bis(4-methoxyphenyl)imidazole

grating. When the electric field is switched off, the EPNA molecules relax back to their random arrangement and the intensity of both beams returns back to its original value (the observed time scale during removal of the electric field is artificial, caused by the slow discharge of the power supply). The space charge field may still exist inside the sample for quite some time, but in the absence of electrooptic effects there is no refractive index change. Reversing the polarity of the applied field causes energy exchange in the opposite direction, due to the fact that the electrooptic coefficient changes sign.

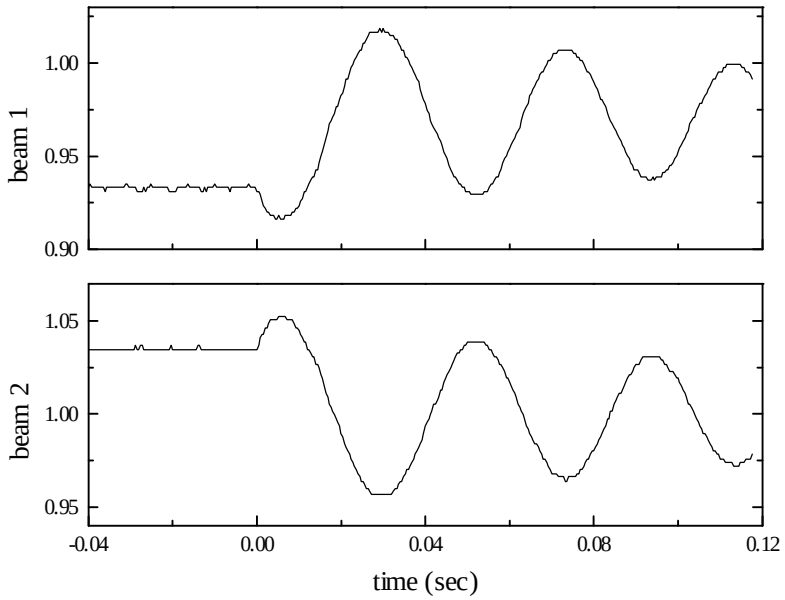

***Fig. 3.9** : The modulation of the transmitted power of the two beams in a PVK:TNF:EPNA sample, due to translation at t=0.0 sec. The electric field was 55 V/μm and translation begun at time equal zero.*

After the presence of a photorefractive grating is established with this simple experiment, quantitative information about its basic properties, the amplitude and phase shift, as well as about the presence of complimentary absorption gratings is acquired with the two beam coupling (2BC) technique. In figure 3.9, a typical trace from a PVK:TNF:EPNA sample is shown. At time equal to 0.0 sec sample translation begins and the signals on the two photodiodes are modulated as the two beams read out the

grating. The two signals are 180 degrees out of phase, indicating the dominance of the refractive index grating[7] . Slight erasure during sample translation is observed.

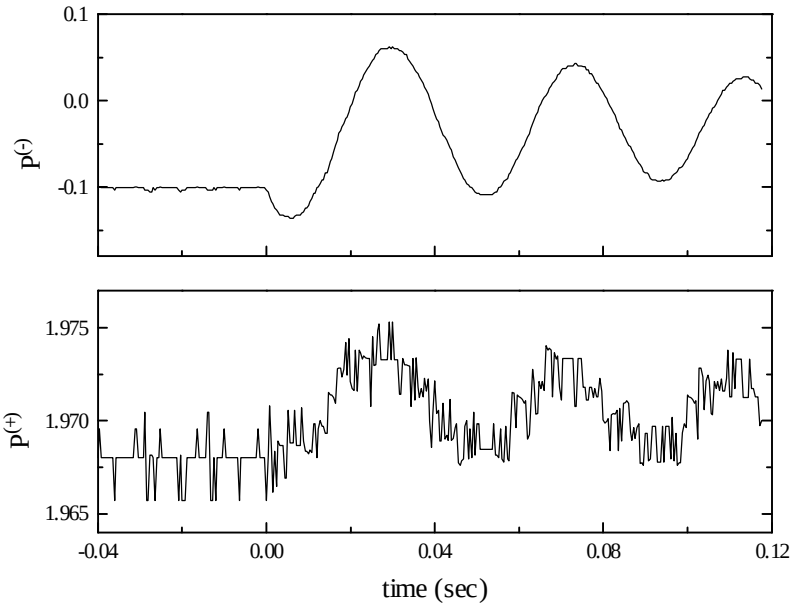

Fig. 3.10 *: The sum $P^{(+)}$ and the difference $P^{(-)}$ of the powers of the two beams plotted in figure 3.9.*

The analysis of the 2BC data is carried out on the basis of the sum $P^{(+)}$ and the difference $P^{(-)}$ of the two signals, which are plotted in figure 3.10. A small modulation in $P^{(+)}$ reveals the presence of a weak local absorption grating[8], with an amplitude that is around 35 times smaller than that of the refractive index one (shown in $P^{(-)}$). Local absorption gratings (which may arise due to the difference in the absorption of the neutral and the ionized charge generating site), often accompany photorefractive ones in inorganic crystals. Their presence has also been reported in a photorefractive polymer and photochromism was suggested as a possible source [35]. The origin of the absorption grating in PVK:TNF:EPNA is not clear at present, however, its amplitude is very small and its contribution to the diffraction efficiency is negligible.

[7] see equations (2.20).

[8] see equations (2.21).

From the 2BC experiment, the diffractive amplitude P of the refractive index grating is revealed to be around 3 cm^{-1} at 55 V/μm applied across the sample. This value was reproducible from spot to spot on the same sample within 10%. The corresponding refractive index is given by[9]:

$$\Delta n = P/(\pi\cos(\vartheta_2-\vartheta_1)/\lambda_0(\cos\vartheta_1\cos\vartheta_2)^{1/2}) \quad (3.4)$$

and it is found to be in the order of $4\cdot10^{-4}$. Another important parameter that can be estimated from the 2BC experiment is the diffraction efficiency[10]:

$$\eta \approx (Pd)^2 \quad (3.5)$$

which reaches a value in the order of 0.1%, at 55 V/μm. The same value was measured with DFWM. This diffraction efficiency may seem low, compared to almost 100% which has been demonstrated in inorganic photorefractives [36]. However, the thickness of the polymer is only 100 μm and its properties are far from optimized. With efficient plasticization, a diffraction efficiency of almost 100% has also been observed recently in a PVK based photorefractive polymer [16].

A very important quantity that is revealed with the 2BC experiment is the phase shift of the refractive index grating. According to the standard model for photorefractivity, φ tends towards π/2 in the region of high applied electric fields. The data of figure 3.10, reveal a value for φ which is around 40 degrees. Before considering an explanation on the basis of the standard model, let us examine an alternative scenario: In the case where a local, unknown origin refractive index grating coexists with a π/2 phase shifted photorefractive one with approximately the same amplitude, the 2BC experiment (which would measure the first Fourier component of the sum of these two gratings) would yield a phase shift around 45 degrees. This local grating has to be electric field dependent and reversible, otherwise it would be detected during write and read-out experiments, but it should have a different time constant[11].

According to this scenario, the decay of the diffraction efficiency should consist of two components, with approximately equal amplitude and different response time.

---

[9] see equation (2.13).

[10] see equation (2.14).

[11] It is very hard to imagine a complimentary refractive index grating other than photorefractive, which is electric field dependent and has the same response time as the photorefractive one.

This is clearly not the case in figure 3.11, where the diffraction efficiency in PVK:TNF:EPNA is shown to decay in a single exponential fashion. The line is a fit according to the standard model for photorefractivity[12] :

$$\eta(t) \propto (E_{SC}(0)\exp(-t/\tau))^2 \qquad (3.6)$$

where $E_{SC}(0)$ is the steady state value of the space charge field. Form the above picture it is clear that only one grating exists inside the sample. Its response time constant τ was found to decrease with increasing TNF concentration, applied electric field and light intensity.

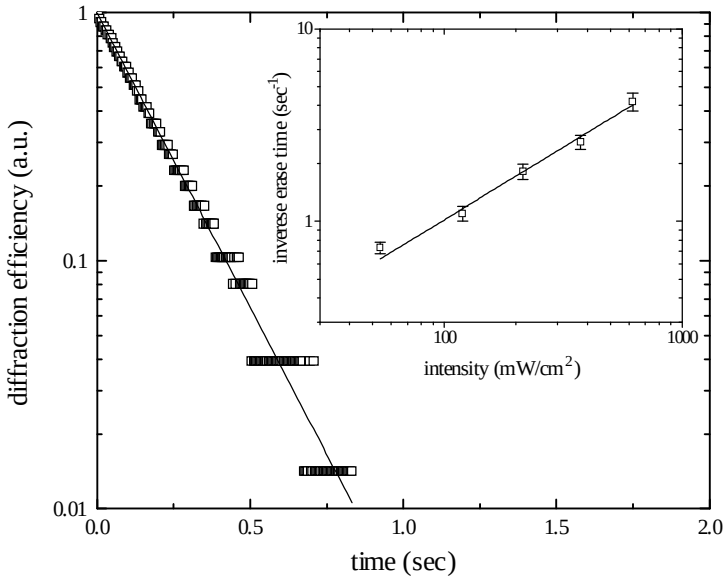

Fig. 3.11 *: Erasure of the photorefractive grating in a PVK:TNF:EPNA sample. The voltage on the needle was 10 kV and the sample was 65 μm thick. The beam intensity was 600 mW/cm^2 outside the sample. The line is a fit to equation (3.6), with τ=183 msec. Inset : The dependence of inverse response time constant τ^{-1} on the erasing beam intensity for the EPNA composite. The electric field was 55 V/μm.*

[12] see equations (2.11) and (1.10).

In the inset of figure 3.11, the inverse response time constant τ^{-1} is shown for various intensities of the erasing beam. Although a linear dependence would fit the data rather good, a power law is commonly used in literature. The reason for this is that shallow traps, which are expected to occur naturally in polymers[13], cause a sublinear dependence of τ^{-1} on intensity. This has been firstly demonstrated in $BaTiO_3$ [37] and has been also observed in several photorefractive polymers [3,10,13]. Accordingly, the line in figure 3.11 is a fit to a power law, yielding an exponent of 0.7±0.3. The large error is due to the limited range of the measurement, which is set by the maximum intensity which is available from the laser and the dark erase time. Although no definite conclusion can be drawn from this fit concerning the presence of shallow traps, their density should not be very high, otherwise it would cause a derivation from the exponential decay of diffraction efficiency versus time [38].

Let us consider the electric field dependence of the amplitude and the phase shift of the photorefractive grating and discuss it within the standard model for photorefractivity. This model was developed to describe the space charge field formation in inorganic photorefractive materials and subsequently, when it comes to polymers, several distinct characteristics are ignored: The mobility and the efficiency of charge generation for example are highly electric field dependent in polymers. Moreover, the nature of trapping sites is not known and their density may as well be field dependent. Despite these deficiencies, the physical picture of the space charge field formation in polymers is very similar with that in inorganic materials. Since the equations on which the model is based are very general, it should still be able to predict trends and give reasonable order-of-magnitude estimates in the steady state regime.

According to this model, the space charge field, in the case where the diffusion field is ignored[14], is given by[15]:

$$E_{SC}=mE_K[1+(E_K/E_S)^2]^{-0.5} \qquad (3.7)$$

where E_K is the projection of the external field along the grating wave vector and E_S is the saturation field. The space charge field increases in a linear-like fashion for small

[13] this point will be further discussed in chapter four.

[14] In this geometry E_D=0.1 V/μm. However, the Einstein relation between the diffusion coefficient and the drift mobility is believed not to hold in disordered materials [39]. Moreover, from time-of-flight experiments it was shown that charge transport in PVK cannot be described with the introduction of a diffusion coefficient [40]. For this reason, in a first approximation, the diffusion field is ignored.

[15] see equation (1.6).

applied electric fields and reaches saturation when E_K approaches E_S (figure 1.3). The diffractive amplitude of the photorefractive grating depends on the electrooptic coefficient, which increases linearly with electric field and the space charge field[16]:

$$P \propto r_{eff} E_{SC} \tag{3.8}$$

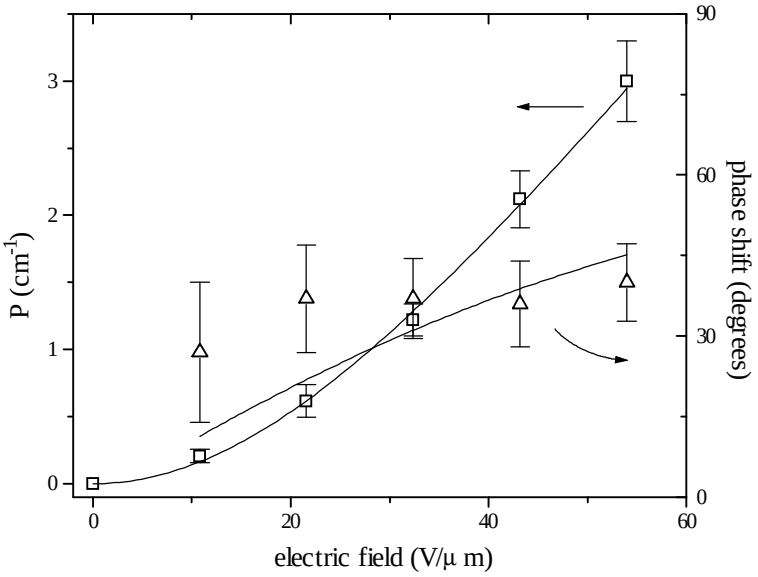

Fig. 3.12 *: The diffractive amplitude P and the phase shift φ of the refractive index grating for PVK:TNF:EPNA, measured with the 2BC experiment on the same spot of the sample. The lines are fits to the standard model for photorefractivity. At 55 V/μm, the value of P showed a variation in the order of 20% from sample to sample, while the variation in φ was up to 40%.*

Thus, a superlinear dependence is expected in the region of small electric fields, followed by a linear increase after the saturation field has been reached. The electric field dependence of P for PVK:TNF:EPNA is shown in figure 3.12. A superlinear dependence indicates that the space charge field is below or close to its saturation value. The line is a fit to equation (3.8), yielding excellent agreement between the standard model and the experimental data for a value of the saturation field equal to 21.5±9

[16] see equation (2.8).

V/μm. This value of E_S, which is comparable to E_K (E_K is equal to 22 V/μm when 55 V/μm are applied across the sample), is rather reasonable. It corresponds to a trap density of $(1.7\pm0.7)\cdot10^{16}$ cm^{-3} (for $\varepsilon=3.5\varepsilon_0$)[17], which is typical for inorganic photorefractive materials. A similar trap density has been recently measured in an other PVK based photorefractive polymer [41]. The origin of these trapping centers is not clear at present; a discussion on this subject can be found in the next chapter.

The space charge field reaches a value in the order of 15 V/μm for 55 V/μm applied across the sample (E_K=21.5 V/μm and m=1). Values in this range, which are typical for photorefractive polymers [2], are rather larger compared with what is usually observed in inorganic photorefractive materials. This comes as a result of the lower dielectric constant of polymers, which allows a higher electric field for the same amount of trapped charge. With this value of the space charge field, an electrooptic coefficient in the order of a few pm/V is needed in order to explain the observed diffraction efficiency.

Since the saturation field is comparable to E_K, intermediate values between 0 and π/2 are expected for the phase shift of the photorefractive grating. According to the standard model, in the case where the diffusion field is ignored, φ is given by[18]:

$$\varphi=\arctan(E_K/E_S) \tag{3.9}$$

In figure 3.12, the calculated dependence of φ is shown for E_K=21.5 V/μm, together with measured values. Considering the simplicity of the model, the agreement is rather satisfactory. The intermediate values of the phase shift can be understood within the standard model as a result of a high trap density, in the order of 10^{16} cm^{-3}. However, this value should be regarded as highly approximate. Substantial scatter is observed in the data, especially among samples from different bunches. The phase shift for example can show variations up to 40%, presumably due to impurities that enter accidentally in the polymer during sample preparation. These variations translate to larger ones for the trap density.

In the above, the discussion was limited to the EPNA composite, as the diffraction efficiency is higher, allowing a better signal-to-noise ratio. The same observations however apply also to the HONB composite. In this case, the diffractive amplitude of the photorefractive grating was roughly four times lower, a value that corresponds to the ratio of the electrooptic coefficients at low frequencies, indicating a comparable magnitude of the space charge field in both composites. The diffraction

[17] see equation (1.8).

[18] see equation (1.6).

efficiency was around 0.006% at 55 V/μm. The phase shift of the HONB samples was slightly higher, indicating that the trap density exhibits a weak dependence on the NLO chromophore. This point will be further discussed in chapter five.

3.2.5. Asymmetric energy exchange in poly(*N*-vinylcarbazole) based photorefractive composites

The gain coefficient Γ is among the most important characteristics of a photorefractive material. Most of the proposed applications rely on the existence of large gain, which surpasses the absorption losses, giving rise to net gain, or amplification of a laser beam propagating through the material. This is shown in figure 3.13 to be the case for the EPNA composite, at electric fields higher than 40 V/μm. The absorption coefficient is plotted on the same graph, indicating the level above which net gain occurs. The HONB composite on the other hand shows no net gain below 80 V/μm due to the lower electrooptic coefficient.

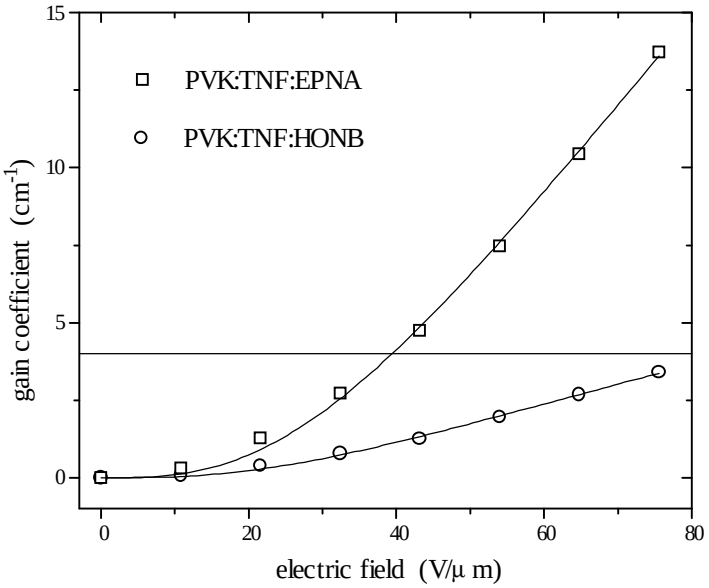

Fig. 3.13 *: The gain coefficient for PVK:TNF:EPNA and PVK:TNF:HONB as a function of electric field. The error bars, which are not shown for clarity, are within 10%. The lines are fits to the standard model. For this experiment* β*=1. The reproducibility of* Γ *from sample to sample was within 20%.*

This superlinear dependence is in agreement with a space charge field below or close to its saturation value and has been observed in other PVK based photorefractive polymers [10,13,16]. According to the standard model, the enhancement of Γ with an applied electric field is through the electrooptic coefficient, the space charge field and the phase shift[19]:

$$\Gamma \propto r_{eff} E_{SC} \sin\varphi \qquad (3.10)$$

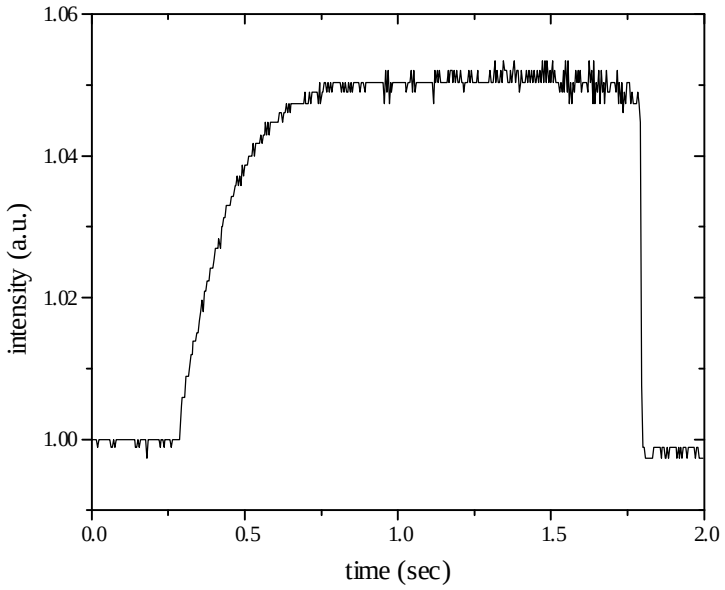

Fig. 3.14 *: The intensity of the probe beam in a PVK:TNF:EPNA sample as the pump is switched on at t=0.3 sec. The pump is blocked at approximately 1.8 sec. The electric field was 65 V/μm.*

The lines in figure 3.13 are fits to equation (3.10), yielding a saturation field equal to 19±1 V/μm for PVK:TNF:EPNA and 16±1 V/μm for PVK:TNF:HONB. The agreement with theory is stunning. The saturation field for the EPNA composite is in agreement with the previously estimated trap density, while for the HONB composite, the latter quantity is around 20% lower. This point will be further discussed in chapter five.

[19] see equation (1.14).

In the casted samples a gain coefficient up to 26 cm^{-1} was achieved for 10 kV on the needle, due to the higher electric field that could be applied before breakdown. Unfortunately, the exact value of the applied electric field during corona poling is not known. Using data from the sandwiched samples however, this value is estimated to be around 155 V/μm, meaning that approximately 80% of the voltage on the needle was applied across the sample during corona poling.

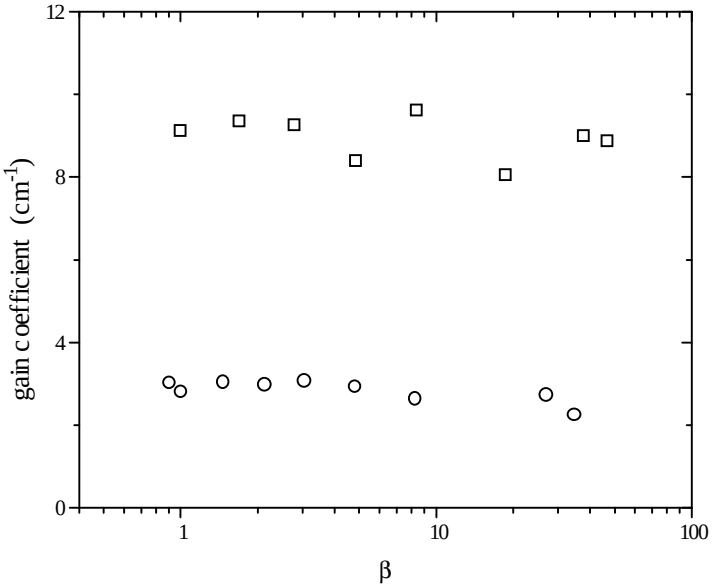

Fig. 3.15 *: The dependence of the gain coefficient of PVK:TNF:EPNA (squares) and PVK:TNF:HONB (circles) on the ratio* β *between the intensity of the pump and the probe beam.*

The temporal behaviour of the energy exchange is shown in figure 3.14, where the intensity of one of the writing beams (probe) is monitored as a function of the presence of the second beam (pump), in a PVK:TNF:EPNA sample. At time ~0.3 sec, the pump beam is instantly switched on and gain is observed in the intensity of the probe. This energy exchange does not take place instantly, but has a finite rise time, associated with the growth of the space charge field. At time ~1.8 sec, the pump beam is switched off and the intensity of the probe beam returns to its initial value. The photorefractive grating persist inside the sample for some time before it is erased and some part of the probe beam is diffracted, but energy transfer seizes instantly, as it requires the presence of both beams.

Finally, the dependence Γ on the ratio β between the intensity of the pump and the probe was investigated. According to theory, the gain coefficient is independent of the modulation index of the photorefractive grating, thus it should be independent of β. This is shown to be true in the case of PVK:TNF:EPNA and PVK:TNF:HONB (figure 3.15), for almost two decades of β. This independence of gain on the modulation index has been also observed in photorefractive inorganic crystals [42] and polymers [10].

3.2.6. The mechanism of the refractive index change

In the standard photorefractive model, the space charge field changes the refractive index via the linear electrooptic effect:

$$\Delta n=-(1/2)n_0^3 r_{eff} E_{SC} \tag{3.11}$$

where r_{eff} is the true linear electrooptic coefficient. However, according to SHG and electrooptic measurements, the NLO molecules in PVK:TNF:EPNA and PVK:TNF:HONB have a substantial degree of orientational mobility at room temperature, giving rise to Kerr effects. During photorefractive grating growth, the NLO molecules are under the influence not only of the external field, but also of the space charge field, which has only a few times smaller magnitude. It is thus tempting to assume that their orientation will be modulated by the space charge field, causing a spatial variation of the birefringence and the electrooptic coefficient. Both these effects can contribute to the refractive index change, leading to an increase of the diffraction efficiency. This mechanism is known as the orientational enhancement of photorefractivity [43].

In order to check whether the mechanism of orientational enhancement is operational in PVK:TNF:EPNA and PVK:TNF:HONB, polarization anisotropy (the ratio between the change in refractive index for *p*- and for *s*-polarized light, Δn_p and Δn_s respectively) measurements can be used. In the case of a pure linear electrooptic effect, the ratio $\Delta n_p/\Delta n_s$ is solely determined by the ratio r_{33}/r_{13} (which is equal to 3 for poled polymers [30]) and it is always positive, even in the tilted geometry used here [43]. This is not true in the case of orientational enhancement: Wu has calculated the change in the refractive index due to an applied electric field, in the simplest case of an ensemble of dipolar, rodlike molecules [44]. The change due to birefringence is:

$$\Delta n_{\parallel}^{(BR)}=C_{BR}E_T^2 \tag{3.12a}$$

$$\Delta n_{\perp}^{(BR)}=-(1/2)C_{BR}E_T^2 \tag{3.12b}$$

and due to the modulation of the electrooptic coefficient is:

$$\Delta n_{\parallel}^{(EO)} = (1/2) C_{EO} E_T^2 \quad (3.13a)$$

$$\Delta n_{\perp}^{(EO)} = (1/6) C_{EO} E_T^2 \quad (3.13b)$$

where $\Delta n_{\parallel}$ and $\Delta n_{\perp}$ are the changes in the refractive index parallel and perpendicular to the electric field and the constants C depend on the temperature, density and molecular parameters of the NLO molecules. E_T is the total electric field, which in the case of photorefractive polymers is the sum of the external and the space charge field.

From equations (3.12) it can be seen that the change of the refractive index due to birefringence reverses sign when measured parallel and perpendicular to the applied electric field. This means that the ratio $\Delta n_p / \Delta n_s$ for a refractive index grating that arises from a spatial variation of the birefringence, will be negative.

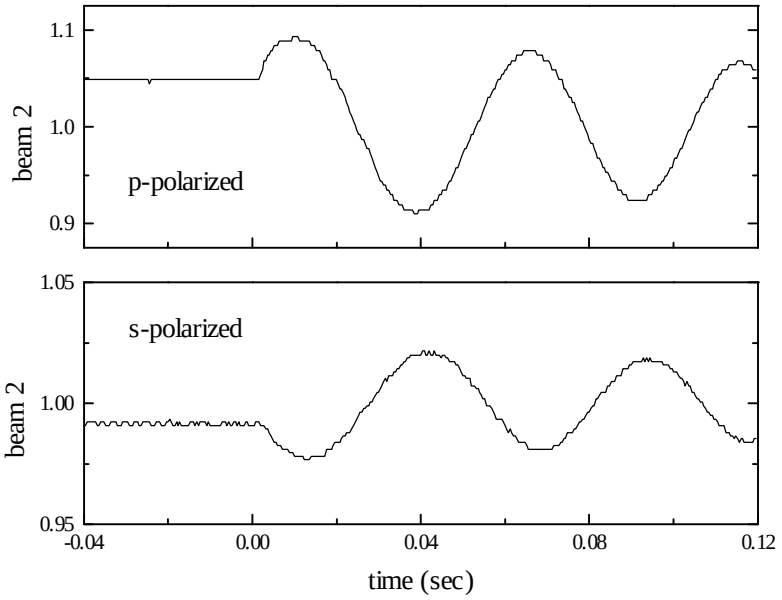

***Fig. 3.16** : Two beam coupling traces from the EPNA composite, for p- and for s-polarized light. Only the second beam is shown in both cases.*

In figure 3.16, the modulation of the intensity of one of the beams during a two beam coupling experiment in the EPNA composite is shown for *p*- and *s*-polarized light. According to theory[20] :

[20] equation (2.20b), with A set to zero.

$$P_2 \propto 2Pd\sin(\varphi_P+2\pi vt/\Lambda_G) \quad (3.14)$$

which means that P and consequently the change in the refractive index Δn reverses sign with polarization, indicating a substantial contribution from the spatial modulation of birefringence. The traces in figure 3.16 clearly demonstrate that the mechanism of orientational enhancement is operational in PVK:TNF:EPNA and PVK:TNF:HONB.

The exact magnitude of the contribution due the modulation of the birefringence and the electrooptic coefficient cannot be estimated without separate measurements. These contributions however are also present in the electrooptic experiments and in this way, the electrooptic coefficient that is measured can be used for order-of-magnitude estimates and comparison of various compounds.

3.3. Conclusions and outlook

In conclusion, by combining the well known photoconductor PVK sensitized with TNF and the NLO molecules EPNA and HONB, two novel polymer composites that exhibit photorefractivity at 633 nm were developed and net gain was measured in one of them. The electrooptic effect in these materials was shown to contain a major contribution from Kerr effects, arising from the substantial orientational mobility of the NLO molecules at room temperature. The standard theory of photorefractivity could describe the electric field dependence of the amplitude and the phase shift of the photorefractive grating and give reasonable order-of-magnitude estimates of important parameters. A trap density in the order of 10^{16} cm^{-3} was estimated for both composites. Finally, the refractive index change in these materials was found to contain a contribution from the spatial modulation of the birefringence due to the reorientation of the NLO molecules in the space charge field.

PVK based composites seem to be promising candidates for efficient photorefractive materials. However, still a lot of things remain to be understood. The nature of the trapping centers in one of them. An approach towards the study of charge trapping in photorefractive polymers is presented in the next chapter.

The mechanical properties of the composites discussed here are clearly not at the optimum and there is substantial room for improvement. The temperature dependence of the electrooptic coefficient for example, suggest that almost a ten fold increase of the diffraction efficiency may take place, if the T_g is lowered close to room temperature with the addition of a proper plasticiser. The existence of the orientational enhancement mechanism hints that the NLO molecule should not be attached to a polymer chain, as this would lead to a decrease of its orientational mobility. The exact magnitude of the contribution due to the modulation of the birefringence and the electrooptic coefficient should be estimated and the NLO molecules designed accordingly.

3.4. References

[1] W.E. Moerner and S.M. Silence, *Chem. Rev.* 94, 127 (1994)

[2] S. Ducharme, J.C. Scott, R.J. Twieg and W.E. Moerner, *Phys. Rev. Lett.* 66, 1846 (1991)

[3] S.M. Silence, C.A. Walsh, J.C. Scott, T.J. Mattray, R.J. Twieg, F. Hache, G.C. Bjorklund and W.E. Moerner, *Opt. Lett.* 17, 1107 (1992)

[4] J.S. Schildkraut, *Appl. Phys. Lett.* 58, 340 (1991)

[5] M. Liphardt, A. Goonesekera, B.E. Jones, S. Ducharme, J.M. Takacs and L. Zhang, *Science* 263, 367 (1994)

[6] H.J. Bolink, V.V. Krasnikov, G.G. Malliaras and G. Hadziioannou, in *Nonlinear Optical Properties of Organic Materials VI, SPIE proc.* 2025, ed. G.R. Möhlmann, San Diego (1993)

[7] L. Yu, W. Chan, Z. Bao and S.X.F. Cao, *Macromolecules* 26, 2216 (1993)

[8] S.M. Silence, D.M. Burland and W.E. Moerner, in "*Photorefractive Effects and Materials*", D.D. Nolte, ed., Kluwer Academic (1995)

[9] Y. Zhang, R. Burzynski, S. Ghosal and M.K. Casstevens, to appear in *Adv. Mater.*

[10] M.C.J.M. Donkers, S.M. Silence, C.A. Walsh, F. Hache, D.M. Burland, W.E. Moerner and R.J. Twieg, *Opt. Lett.* 18, 1044 (1993)

[11] Y. Zhang, Y. Cui and P.N. Prasad, *Phys. Rev. B.* 46, 9900 (1992)

[12] B. Kippelen, Sandalphon, N. Peyghmbarian, S.R. Lyon, A.B. Padias and H.K. Hall Jr., *Elect. Lett.* 29, 1873 (1993)

[13] M.E. Orczyk, B. Swedek, J. Zieba and P.N. Prasad, *J. Appl. Phys.* 76, 4995 (1994)

[14] S.M. Silence, M.C.J.M. Donkers, C.A. Walsh, D.M. Burland, R.J. Twieg and W.E. Moerner, *Appl. Opt.* 33, 2218 (1994)

[15] M.E. Orczyk, J. Zieba and P.N. Prasad, *J. Phys. Chem.* 98, 8699 (1994)

[16] K. Meerholz, B.L. Volodin, Sandalphon, B. Kippelen and N. Peyghambarian, *Nature* 371, 497 (1994)

[17] Du Lei, J. Runt, A. Safari and R.E. Newnham, *Macromolecules* 20, 1797 (1987)

[18] Thanks are due to H.J. Bolink and G.O.R. Alberda van Ekenstein for carrying out the DSC measurements.

[19] A. Dulcic, C. Flytzanis, C.L. Tang, D. Pepin, M. Fitzon and Y. Hoppiliard, *J. Chem. Phys.* 74, 1559 (1981)

[20] J.C. Scott, L. Pautmeier and W.E. Moerner, *Synth. Metals* 54, 9 (1993)

[21] T. Kawakami and N. Sonoda, *Appl. Phys. Lett.* 62, 2167 (1993)

[22] B. Kippelen, K. Tamura, N. Peyghambarian, A.B. Padias and H.K. Hall Jr., *Phys. Rev. B* 48, 10710 (1993)

[23] H.J. Bolink, V.V. Krasnikov, G.G. Malliaras and G. Hadziioannou, *Adv. Mater.* 6, 574 (1994)
[24] G.G. Malliaras, V.V. Krasnikov, H.J. Bolink and G. Hadziioannou, manuscript in preparation.
[25] for a recent review see P.M. Borsenberger and D.S. Weiss, eds. "*Organic Photoreceptors for Imaging Systems*", Optical Engineering vol. 39, Marcel Dekker, Inc. (1993) and references therein.
[26] P.J. Reucroft in "*Photoconductivity in Polymers: an Interdisciplinary Approach*", A.V. Patsis and D.A. Seanor, eds., Technomic (1976)
[27] G. Weiser, *J. Appl. Phys.* 43, 5028 (1972)
[28] W.D. Gill, *J. Appl. Phys.* 43, 5033 (1972)
[29] D.M. Burland, R.D. Miller and C.A. Walsh, *Chem. Rev.* 94, 31 (1994)
[30] P.N. Prasad and D.J. Williams, "*Introduction to Nolinear Optical Effects in Molecules and Polymers*", Wiley Interscience (1991) and references therein.
[31] H.T. Man and H.N. Yoon, *Adv. Mater.* 4, 159 (1992)
[32] A. Dulcic and C. Sauteret, *J. Chem. Phys.* 69, 3453 (1978)
[33] P.K. Wu, G.R. Yang, X.F. Ma, A. Cococziela and T.M. Lu, *J. Appl. Phys.* 77, 2258 (1995)
[34] S.M. Silence, M.C.J.M. Donkers, C.A. Walsh, D.M. Burland, W.E. Moerner and R.J. Twieg, *Appl. Phys. Lett.* 64, 712 (1994)
[35] C.A. Walsh and W.E. Moerner, *J. Opt. Soc. Am. B* 9, 1642 (1992)
[36] see for example P. Günter and J.P. Huignard in "*Photorefractive Materials and their Applications I and II*", P. Günter and J.P. Huignard eds., Topics in Applied Physics vol. 61 and 62, Springer-Verlag (1988)
[37] D. Mahgerefteh and J. Feinberg, *Phys. Rev. Lett.* 64, 2195 (1990)
[38] P. Tayebati and D. Mahgerefteh, *J. Opt. Soc. Am. B* 8, 1053 (1991)
[39] L. Pautmeier, R. Richert and H. Bässler, *Phil. Mag. B* 3, 587 (1991)
[40] H. Scher and E.W. Montroll, *Phys. Rev. B* 12, 2455 (1975)
[41] M.E. Orczyk, J. Zieba and P.N. Prasad, *Appl. Phys. Lett.* 67, 311 (1995)
[42] N.V. Kukhtarev, V.B. Markov, S.G. Odulov, M.S. Soskin and V.L. Vinetskii, *Ferroelectrics* 22, 961 (1979)
[43] W.E. Moerner, S.M. Silence, F. Hache and G.C. Bjorklund, *J. Opt. Soc. Am. B* 11, 320 (1994)
[44] J.W. Wu, *J. Opt. Soc. Am. B* 8, 142 (1991)